N-Degradomic analysis reveals a proteolytic network processing the podocyte cytoskeleton

Markus M. Rinschen [#1,2,3,4], Ann-Kathrin Hoppe [1,2], Florian Grahammer [5,6], Martin Kann [1,2], Linus A. Völker [1,2], Eva-Maria Schurek [1,2], Julie Binz [1,2], Martin Höhne [1,2,3,4], Fatih Demir [7], Milena Malisic [7], Tobias B. Huber [5,6,8], Christine Kurschat [1,2], Jayachandran N. Kizhakkedathu [9], Bernhard Schermer [1,2,3,4], Pitter Huesgen*[# 7], Thomas Benzing*[# 1,2,3,4]

1 Department II of Internal Medicine, University of Cologne, Cologne, Germany
2 Center for Molecular Medicine Cologne (CMMC), University of Cologne, Cologne, Germany
3 Cologne Excellence Cluster on Cellular Stress Responses in Aging Associated Diseases (CECAD), University of Cologne, Cologne, Germany
4 Systems Biology of Ageing Cologne (Sybacol), University of Cologne, Cologne, Germany
5 Department of Medicine IV, Medical Center and Faculty of Medicine, University of Freiburg, Germany
6 III. Medizinische Klinik, Universitätsklinikum Hamburg-Eppendorf, Hamburg, Germany
7 Central Institute for Engineering, Electronics and Analytics, ZEA-3, Forschungszentrum Jülich, Wilhelm-Johnen-Str, 52425 Jülich, Germany
8 Center for Systems Biology (ZBSA), Albert-Ludwigs-University, Freiburg, Germany
9 Centre for Blood Research, Department of Pathology & Laboratory Medicine, Department of Chemistry, 2350 Health Sciences Mall, University of British Columbia, Vancouver V6T 1Z3, Canada

* Shared senior authorship

Address correspondence to

University Hospital Cologne
Kerpener Str. 62, 50937 Köln, Germany
Phone.: +49 221 478-4480
Email: markus.rinschen@uk-koeln.de or thomas.benzing@uk-koeln.de

Or
ZEA-3 Analytics, Forschungszentrum Jülich
Wilhelm-Johnen-Str, 42425 Jülich, Germany
Phone: +49 2461 61-6873
Email: p.huesgen@fz-juelich.de

Author version of the manuscript.
Published in J Am Soc Nephrol. 2017 Oct;28(10):2867-2878.
doi: 10.1681/ASN.2016101119.

Abstract

Regulated intracellular proteostasis and proteolysis is essential in maintaining the integrity of podocytes and the glomerular filtration barrier of the kidney. Altered proteolytic substrate turnover has been associated with various glomerular diseases ranging from diabetic nephropathy to focal and segmental glomerulosclerosis. However, to date it has not been possible to systematically identify proteolytically cleaved proteins although some of the proteases have been characterized. Here we applied a novel proteomics technology that enables proteome-wide identification, mapping, and quantification of protein N-termini to comprehensively characterize cleaved podocyte proteins in the glomerulus *in vivo*. We found evidence for many previously undescribed proteoforms of important podocyte proteins. Among others, podocin, nephrin, neph1, alpha-actinin and vimentin exist as various proteoforms resulting from defined proteolytic cleavage. Quantitative mapping of N-termini demonstrated perturbation of protease action during podocyte injury in vitro, including diminished proteolysis of alpha-actinin-4. Differentially regulated protease substrates were cytoskeletal proteins, including actin-associated proteins, but also intermediate filaments. We determined preferential protease motifs during podocyte damage which indicated that caspase proteases are activated, and arginine-specific proteases are inhibited during podocyte damage. Several regulation processes were clearly site-specific, conserved across species, and could be confirmed by differential migration behavior of protein fragments in gel electrophoresis. Some of the proteolytic changes discovered in vitro were also found in two *in vivo* models of podocyte damage (WT1 heterozygous knockout mice and PAN-treated rats). Taken together, we provide first direct and systems-level evidence that both slit diaphragm and podocyte cytoskeleton are regulated targets of proteolytic modification, which is further dynamically altered upon damage.

Main Text

The majority of kidney diseases start in the glomerulus due to the susceptibility of the renal filtration unit to metabolic, genetic, mechanic and immunological damage. The glomerular filtration unit consists of three layers, fenestrated endothelial cells, the glomerular basement membrane and podocytes [1]. Podocytes are terminally differentiated, interdigitating cells that engulf the glomerular capillaries [1]. Damage to these cells results in proteinuria [1,2]. Genetic studies have identified essential podocyte proteins which maintain the barrier. Mutation of these genes leads to altered signaling cascades in glomerular diseases and to FSGS. [2] . Of critical importance are membrane proteins, such as podocin and nephrin [3,4] and cytoskeletal proteins such as alpha-actinin-4 (ACTN4) [5].

Proteolytic processing is an irreversible, site-specific protein modification that regulates essential physiological processes by generating protein isoforms (proteoforms) and controlling proteostasis [6]. Deregulated proteolysis is a key driver for human diseases, and proteases are promising targets for tailored therapeutics [7]. Recent studies indicated that maintenance of the renal filtration barrier largely relies on proteases as key regulators of podocyte function, including Cathepsin D, Cathepsin L and matrix metalloproteases [8–11]. High copy numbers of intracellular proteases with broad specificity are found in the podocyte transcriptome and proteome, and they accumulate in disease states [12] [8,9,13,14]. Although essential proteases and a few of their targets have been identified, it is largely unclear which particular podocyte proteins are cleaved, which proteoforms are generated at which site(s), and how proteolytic cleavage affects their physiological function in health and disease. Distinction of processed and precursor proteins is challenging by standard proteomics because many tryptic peptides are shared by both proteoforms, whereas the informative protease-generated neo-terminal peptides constitute only a very minor fraction that is rarely identified [15]. Here, we overcome this limitation using the innovative Terminal Amine-based Isotope Labeling of Substrates (TAILS) technique, a strategy enabling site-specific mapping of protease-generated novel protein termini ("degradomics") [16–18]. The aim of this first unbiased, systems level study of podocyte degradomics was to delineate proteolytic protein modifications and demonstrate dynamic proteolytic regulation of cytoskeletal proteins in injury.

To obtain an atlas of proteolytically cleaved proteins in podocytes of living animals we applied the TAILS technology combined with mass spectrometry based protein identification. Technical precautions were taken to minimize *ex vivo* proteolysis by harvesting freshly isolated mouse glomeruli with a comprehensive protease inhibitor cocktail and performing protein isolation rapidly at cold temperatures (see methods). In the first steps of the TAILS procedure, proteins were denatured and primary amines (e-amines of Lys side chains; a-amines of native, unmodified amino (N-) termini and protease-generated neo-N-termini) modified by reductive dimethylation [18] (Fig. 1A). Hence, all N-termini were either modified by endogenous modifications such as acetylation, or *in vitro* by dimethylation (Fig. 1A).

Next, tryptic digest was performed and N-terminal peptides were enriched (see methods for details). Proteomic analysis of two such enriched samples from mouse glomeruli identified a total of 3815 N-termini, of which 2976 were modified by dimethylation in vitro while 784 were endogenously acetylated (55 were detected both in acetylated and dimethylated form, Fig 1B, Supplemental Table S1). We mapped these to their topology and classified them depending on their positional annotation: 1343 were “expected” termini, of which 720 started with intact or removed initiation methionine (P1,P2), 6 termini mapping to known alternative transcription start sites, and 521 termini matching to known or predicted sites for signal- or propetide removal (Fig. 1B). 96 termini were annotated as previously described cleavage sites associated with known proteases. Cathepsin D cleavage sites were markedly overrepresented in the dataset as compared to all other known cleavage sites (Fig. 1C). 2448 termini mapped to “unexpected” positions, indicative of extensive proteolysis in podocytes *in vivo*. The vast majority (91%) of unexpected termini was localized outside known protein domains.

We found novel termini in the slit diaphragm proteins podocin (**Fig. 1D**), nephrin, neph1 (Kirrel) (Fig. S1 A) and sites in podocyte cytoskeleton proteins (Fig. S1B). Immunoblot analysis with two antibodies targeting two different epitopes validated the presence of a podocin fragment with approximately 34 kDa, in both glomerular preparations and lysates of fresh, snap-frozen kidney (*ex-vivo* time: <10 s) (Fig. 1D). The presence of podocin at the molecular weight of 34kDa was also confirmed using in-gel digestion and mass spectrometry (Fig. S1C). This is consistent with a stable podocin proteoform comprising only amino acids 59 to 385 as indicated by the observed neo-N-terminus starting with Ala59 (Table 1, Fig. 1D). The 34kDa band was observed in both human and mouse glomeruli (Fig. 1E) and is therefore not the previously described short podocin isoform specific to humans (and not expressed in mice) with a similar molecular size [19]. Interestingly, this podocin cleavage site is associated with a polymorphism in the human sequence with unknown pathogenicity [20] (Fig. 1F). Three of the cleavage sites observed in nephrin and ACTN4 were located in the close vicinity to twelve described mutations leading to hereditary nephrotic syndrome and/or FSGS (Fig. 1F).

To test whether proteolytic processing is altered in podocyte damage, we challenged cultured human podocytes with puromycin aminonucleoside (PAN, 50µg/mL, 24h), an artificial yet well-established model of podocyte injury [21,22] , and performed quantitative TAIL analysis. Immunofluorescence analysis demonstrated the expected typical rearrangement of actin stress fibers but also partial rearrangement of the intermediate filament vimentin (Fig. S2A) [23]. Podocyte viability as measured by XTT assay was not altered by PAN at this timepoint (Fig. S2B). The PAN-treated and vehicle treated proteomes were isolated and labeled with two distinct stable isotope variants of formaldehyde to allow quantification of protease-generated neo-termini (Fig. S2C, *n=4*). After TAILS enrichment we identified a total of 3085 N-termini (Fig 2A). 1665 termini were expected, (P1,2). 235 of the termini resulted from signal- or propeptide removal, and 1123 were unexpected (Fig. 2A), the

majority occurring outside of protein domains. 45 termini occurred precisely at known cleavage sites which are predominantly processed by granzymes and cathepsins (Fig. S3A). Compared to homologous proteins observed in the glomeruli dataset, most cleavages occurred at conserved, identical protein residues or closely adjacent to them, highlighting the highly regulated, site-specific nature of the proteolytic events (Fig. S3B, Table 1).

We could reproducibly quantify 666 N-termini by the log2 normalized ratios of PAN-treated versus control podocytes, as determined from the stable isotope labels. We ranked them according to the ratio and divided them into 10 percentiles (Fig. 2B). Gene-ontology (GO) enrichment analysis of the most strongly increased (Q10) and most strongly decreased (Q1) N-termini showed decreased generation of N-termini on proteins associated with the cytoskeletal organization (Fig 2C), while N termini of proteins with structural activity and general cellular functions were increased upon PAN treatment. To test whether different classes of the cytoskeletal proteins are differentially regulated, we visualized the ratios of neo-termini in different classes of cytoskeletal proteins in cumulative histograms (Fig. 2D, Fig. S4). Surprisingly, unexpected termini of actin-binding proteins were significantly decreased as compared to all other termini (Fig. 2D). Also neo-termini of tubulin and adhesion proteins were decreased, whereas cleavage of mitochondrial proteins was increased (Fig. S4). For ACTN4, an actin-binding protein, we observed a decrease of cleavage between C-terminal EF domains and the Spectrin domains (Fig. 2E). Using a C-terminal polyclonal antibody, we detected two bands corresponding to the apparent molecular mass of ACTN4 proteoforms which were, consistent with our TAILS data, decreased by PAN treatment (compared to the P0 form, Fig. 2F). The large cytoskeletal protein MYH9 exhibited a ladder-like staining indicative of the complex proteolytic pattern with many termini observed for these proteins (Fig. S5 A,B).

To infer quantitative protease hierarchies from the data, we generated motif logos [24] of the top (Q10) and bottom (Q1) percentile to determine whether specific proteolytic activities are affected by PAN challenge (Fig. 3A). The algorithm generates position weighted matrices of overrepresented amino acids surrounding aligned cleavage sites inferred from the neo-termini. In Q1 (decreased N-termini), an R - T cleavage motif was overrepresented as compared to the non-changed N-termini population, indicating that Arg-specific proteases such as trypsin-like serine proteases might be inhibited (Fig. 3A). This class is expressed in podocyte transcriptome but poorly studied [12]. In the strongly induced quantile Q10 we observed an overrepresentation of an aspartate-rich A/D-X-X-D motif preceeding the cleavage site (Fig. 3B). This is the typical motif of the caspases. Consistently with this motif analysis, caspase 3/6 activity was transiently induced by PAN (Fig. 3C) consistent with previous results [22,25]. Interestingly, protease network analysis [26] of observed cleavage sites revealed known downstream targets of caspase 3 including further proteases, but also vimentin and mitochondrial proteins (Fig. 3D, S4D). Vimentin, a key structural component of intermediate filaments, is very abundantly expressed in native and cultured podocyte proteins and transcripts [12]. Degradomics demonstrated

that vimentin was cleaved at D85 upon PAN treatment (Fig 3E). Consistently, a C-terminal, but not an N-terminal antibody identified a band corresponding to the molecular weight of 42 kDa (P1, Fig. 3F), which was reproducibly increased by PAN treatment. Conversely, an N-terminal, but not a C-terminal antibody detected a presumably N-terminal protein fragment decreased by PAN treatment (P2, Fig. 3F).

Finally, we asked whether the proteolytic changes defined by degradomic analysis *in vitro* could be also found *in vivo*. To this end, we analyzed proteolytic cleavage in an *in vivo* model of rat PAN injury by initial degradomics studies. We identified 1334 N-termini, and quantified 552 termini in at least two biological replicates. We observed a large number of proteolytic cleavage products (dimethylated peptides) belong to proteins annotated as “extracellular” or “secreted”. This can be explained by action of proteases on both the serum proteins (e.g. complement) and the extracellular matrix compartment (Fig. 4A). However, we also found that identical, conserved protease cleavage sites on intracellular proteins are regulated in both in vivo and in vitro PAN damage models. For instance the proteolytic cleavage of Vimentin was detectable in all three species and reduced in both in vitro and in vivo PAN model (Fig. 4B). This could be corroborated by immunoblotting: Proteolytically processed vimentin (stained by the N-terminal antibody) was reduced using an N-terminal antibody in PAN rats, similar to cell culture (Fig. 4C). We also found that ACTN4 proteolytic processing was decreased, similar to the effect in human cells (Fig. 4D). To further strengthen the data, we analyzed a non-chemical model of focal segmental glomerulosclerosis: in isolated glomeruli from proteinuric WT1 heterozygous mice, we found decrease of ACTN4 cleavage compared to wildtype littermates (Fig. 4E). Immunoblotting for vimentin showed a “ladder-like” staining in immunoblotting of lysates from WT1 heterozygous mice glomeruli (Fig. S6). These experiments demonstrate the relevance and transferability of the TAILS analyses to the *in vivo* situation.

Conceptually, the method used here is the counterpart to studying kinase substrates and signaling via phosphoproteomics, a method that has provided considerable insights into both glomerular and tubular pathophysiology [27–31]. On a cell biological level, protease processing appears dominant over alternative splicing or transcription start sites (Fig. 1A, 2A). It is intriguing to speculate that some of the stable fragments might exhibit a cellular signaling function as described e.g. for the polycystin-1 C-terminal tail [32]. The results of the quantitative “proof of concept” study are consistent with the current paradigm that cytoskeletal rearrangement is essential for podocyte injury [21,23]. Yet, the findings could be partially explained by the fact that cytoskeletal proteins are extremely high abundant in cultured podocytes and particular amenable to mass spectrometry analysis [33,34]. In conclusion, this study proves the existence of high-stoichiometric protein termini and specific proteolytic machineries which mediate stress-induced processing of crucial components of podocyte structure and biology. These comprehensive results are also available now for further studies.

Concise Methods.

Glomerular preparation and mice.

Male mice (age 8 weeks, 100% BL6N background) were killed by cervical dislocation and kidneys were perfused with magnetic beads to isolate glomeruli as previously described with modifications [27]. Briefly, a solution containing 200µl tosyl-activated Dynabeads dissolved in 10mL ice-cold HBSS with 1X protease inhibitor (Roche) was generated. Mice were decapitated, and kidneys were immediately removed and perfused with the solution. Glomeruli were minced and pressed through a sieve (mesh size 100µm) twice and collected by a magnet, and spun down. Tissue was snap-frozen immediately after pelleting (1min, 3000g) and removal of the supernatant. The mouse holding was done in the University of Cologne animal facility, according to standardized specific pathogen-free conditions. The experimental protocol was examined and approved by the LANUV NRW (Landesamt für Natur, Umwelt und Verbraucherschutz Nordrhein-Westfalen/State Agency for Nature, Environment and Consumer Protection North Rhine-Westphalia).

Cell culture

Human podocytes generated by Saleem et al. [35] were cultured at 33 degrees Celsius in RPMI medium containing 10% FBS and 1x insulin-transferrin supplement (Gibco). Differentiation was induced by culturing podocytes at 37 degrees for 10 days. Cells were treated with PAN dissolved in H2O (final concentration 50µg/mL) and appropriate vehicle controls were performed. No cross-contamination of this cell line with other cell lines is currently reported. The cell cultures were regularly tested negative for mycoplasma.

Proteome preparation.

Podocyte were scratched from the dishes and proteins were dissolved in urea. Acetone precipitation was performed and pellets were washed three times with ice-cold methanol. Then, pellets were dried and resuspended with 1mL 6M GHCl and HEPES 200mM, pH 7.5 with a protease inhibitor cocktail, snap frozen in liquid nitrogen and stored at -80°C until further processed. Glomeruli were processed in an identical fashion.

Terminal Amine Labeling of Substrates (TAILS).

TAILS was performed essentially as described [18] using ca 1 mg/channel proteome as start material. Briefly, proteome samples were thawed, purified by chloroform/methanol precipitation to remove potentially interfering amine-containing compounds, reduced with 10 mM DTT at 65°C for 30 min, alkylated with 25 mM iodoacetamide for 1 h RT in the dark and amine modified by reductive dimethylation [36] using 20 mM sodium cyanoborohydride and 20 mM formaldehyde at 37°C overnight. For PAN-treated proteome, heavy formaldehyde ($^{13}CD_2O$) was used. Reagent addition was repeated and the reaction incubated for another 2h. For the

quantitative experiments, PAN and control proteomes were combined at this point. Samples were then purified by chloroform/methanol precipitation and digested with trypsin (proteome: enzyme ratio 100:1 w/w) at 37°C overnight. Trypsin addition was repeated at 1000:1 (w/w) and digest efficacy controlled using a silver-stained SDS-PAGE gel. A small aliquot of 20 ug proteome was saved as “pre-TAILS control”. Next, dialyzed HPG-ALD (ratio 1:5 proteome:polymer, w/w) and 20 mM sodium cyanoborohydride were added to link bind C-termini and internal peptides. The reaction was allowed to proceed for 2 h at 37°C, then additional 20 mM sodium cyanobrohydride were added, followed by incubation overnight. The polymer was removed by ultra-filtration using spin filter devices (10 mW cut-off, Merck) and the flow-through containing protein N terminal peptides collected.

nLC-MS/MS

Samples were desalted using home-made C18-Stop-And-Go solid phase Extraction tips as described [37]. Peptides were separated on a nano-LC- (2.5h Gradient) , run on a Q Exactive MS/MS (Thermo) coupled to a nano-LC-MS/MS exactly as previously described [38]. For the in vivo TAILS, an estimated 1µg of desalted enriched N-termini peptides were separated on a Ultimate 3000 RSLCDnano HPLC (Thermo) operated in a two-column setup (Acclaim PepMap 100 C18, particle size 3µm, ID 75µm, trap column length 2cm, analytical column length 25cm, Thermo) using a 60 min gradient (2% CAN to 30% CAN(at a flow rate of 300 nl/min. The nanoLC system was on-line coupled to an Impact II high resolution Q-TOF (Bruker) via a CaptiveSpray nano ESI source (Bruker) essentially as described [39]. Nitrogen gas flow in the emitter device was saturated with acetonitrile as dopant using a nanoBooster device (Bruker) MS1 spectra with a mass range from m/z 200 to 1600 wer acquired at 4 Hz, with the Top 15 most intense peaks selelcted for MS/MS analysis using an intensity-dependent spectra acquisition time between 2 and 20 Hz and stepped collision energy (5.6 eV and 8.4 eV for 50% of the acquisition time).

Analysis of nLC-MS/MS Data

Spectra were matched to peptide sequences at a false discovery rate of 0.01 using the Andromeda algorithm [40] as implemented in the MaxQuant Software package v.1.5.3.30. Glomeruli datasets were searched against the UniProt mouse proteome (release 2015_10) with enzyme specificity set as semi-specific (free N-terminus) ArgC, Cys carbamidomethylation and Lys dimethylation (+28.031300) as fixed modifications and var N-terminal dimethylation (+28.031300), N-terminal acetylation (+42.010565) or N-terminal pyroGlu formation from Glu (-18.010565) or Gln (-17.026549).

For PAN-challenge experiment data, similar searches against the Uniprot human proteome (release 2015_10). However, we noted that in the employed version of MaxQuant endogenously N-terminally modified peptides were only unreliably quantified if an N-terminal dimethyl label was defined. As a workaround, datafiles were duplicated and defined as two groups that were searched using mutually

exclusive search parameters. Both parameter sets used semi-specific (free N-terminus) ArgC as digestion enzyme specificity, Cys carbamidomethylation as fixed and Met oxidation as variable modifications and isotope labeling by light (+28.031300) or heavy (+34.063117) dimethylation of Lys residues. The first parameter set additionally required light (+28.031300) or heavy (+34.063117) N-terminal dimethyl labeling for the identification of natural and protease-generated termini with unblocked alpha amines. The second parameter set considered variable N-terminal acetylation (+42.010565) or N-terminal pyroGlu formation from Glu (-18.010565) or Gln (-17.026549), covering endogenously blocked termini and internal peptides carried over by incomplete coupling to the polymer (present as unmodified peptides) or pyro-glu formation. For the dataset from PAN treated rats, these two parameter groups defined above were applied in two independent searches against the Uniprrot rat proteome (release 2015_10 using MaxQuant v 1.5.6.5. In all searches, the PSM FDR was set to 0.01 and the "requantify" option was engaged. All search results were additionally filtered by removing potential contaminants, reverse entries, peptides not ending with Arg as expected from digestion of dimethylated proteins with trypsin, after which the peptide FDR as estimated from the number of reverse entries retained was <0.01 . For quantitative analysis, reverse hits were removed as well as peptides that were not quantified in at least 2 biological replicates.

Further bioinformatics analysis of TAILS Dataset

For all quantified peptides the median of the normalized log2-transformed ratios was calculated. The distribution of median log2-ratios was further divided in 10 quantiles. N-terminal pyro-Glu formation from Gln and Glu is a known side reaction that can occur non-enzymatically at physiological pH in and the vitro during the sample preparation. Hence all peptides with N-terminal pyro-Glu were not considered as native N termini, similar to internal peptides with unmodified N termini that escaped polymer capture.

Information on the termini sequences, matched proteins and positional information were obtained from the MaxQuant output files. Termini were further annotated using the TopFIND Explorer software as implemented in the web portal (clipserve.clip.ubc.ca/topfind/topfinder) [26,41]. A binary decision tree was used for classification: Terminus maps to position 1 (P1) or 2 (P2) in the corresponding protein sequence (YES/NO). If NO: Terminus starts after cleavage of Signal peptide (YES/NO). If NO: Known cleavage (YES/NO). If NO: Alternative transcription start site (YES/NO) If NO: unexpected terminus, inside domain (either P1-P1' or P1' to END) (YES/NO). If NO: unexpected terminus, outside domain. Further bioinformatics analyses were performed using Perseus v. 1.5 [42]. Data were ranked according their ratio (PAN/veh) and GO terms were enriched using the Perseus software using a Fishers exact test (p-values were controlled at FDR <0.05) [42]. Proteins were classified in "actin binding", "cytoskeleton", "microtubule", "cell adhesion" and "Mitochondrion" using the respective uniprot keywords. A Kolmogorov-Smirnoff-test (two way) was performed to delineate differences in distributions between the

proteins annotated with the respective key word and all other proteins. Homologous sites (between mouse and human) were determined by a modified CPHOS software using the termini as an input [43]. This software uses the NCBI homologene groups for alignment across species. A binary decision tree was to determine extracellular proteins. First proteins were filtered for uniprot keyword “secreted” (YES/NO). If NO: Protein is annotated with GO-CC term “extracellular region, extracellular region part, extracellular space, extracellular matrix, extracellular matrix part”. These proteins were determined as “extracellular”. All remaining proteins were determined as “other proteins”.

Raw data deposition

The raw data associated with this study were made publically available at PRIDE /ProteomeExchange (http://www.ebi.ac.uk/pride) PXD005139 Username: reviewer46073@ebi.ac.uk Password: K47R0TZR and Project accession: PXD005140 Reviewer account details: Username: reviewer63512@ebi.ac.uk Password: LGG1rfEm

Human Samples

Unaffected kidney regions from male patients at the age of 60-80) were obtained from nephrectomy surgeries. Written informed consent was obtained from the patients the day before the surgery. All procedures were according to the declaration of Helsinki. The procedure was approved by the local ethics committee. Glomeruli were isolated by sieving with differently sized meshes. Glomeruli were put on ice and then directly snap-frozen in liquid nitrogen.

Immunoblot

Samples from mouse and human glomeruli and from podocyte cells were lysed in 2% SDS buffer and denatured by DNA shreddering by sonication and boiling. Samples were reduced with DTT and run on a 9, 10 or 12 % SDS Gel by gelelectrophoresis, and blotted onto a PVDF membrane by semi-dry transfer. Membranes were blocked with 1x Rotiblock (Roth) for 1h at room temperature and incubated with the primary antibody at a 1:1000 dilution (please see antibodies section) over night. After washing with PBST buffer, blots for mouse and rabbit antibodies were decorated using fluorescence labeled antibodies (IR Dyes, Licor) 1:25000 and developed using a Licor Odyssey imaging system. Blots for goat antibodies were decorated using a horseradish coupled antibody and developed using enhanced chemoluminiscence in a Fusion imaging system.

Podocin immunoprecipitation and in gel digestion

For immunoprecipitation, human glomeruli were lysed in ice-cold IP buffer and homogenized using a glass douncer. The IP buffer used contained 1% Triton X-100; 20 mM Tris pH 7.5; 25 mM NaCl; 50 mM NaF; 15 mM Na4P2O7; 1 mM EDTA; 0.25 mM PMSF; 5 mM Na3VO4). Lysates were precleared with protein G beads. Supernatants containing equal amounts of total proteins were incubated for 1 h at

4°C with anti Podocin antibody (Sigma) and 40µl of Protein G beads. The beads were washed three times with IP-buffer and bound proteins were resolved by 10% SDS-PAGE. One half of the sample was analysed by in-gel tryptic digestion, Stage-tip and nLC-MS/MS analysis exactly as previously described [19]. The other half of the sample was subjected to immunoblotting.

XTT cell viability assay

XTT (2,3-Bis-(2-Methoxy-4-Nitro-5-Sulfophenyl)-2H-Tetrazolium-5-Carboxanilide) cell viability assay (Biotium, Hayward, CA) was performed according to the manufacturer's instructions. 2h of incubation with XTT assay solution was performed in living cells before measurement of XTT uptake using a plate reader (Perqin Elmer) set up according to the manufacturer's instructions.

Reagents

PAN was obtained from Santa Cruz (CAS Number 58-60-6), was dissolved in water. Cytochalasin CAS 22144-77-0 was obtained from SIGMA and dissolved in DMSO (1M). Appropriate vehicle controls were used. The HPG-ALD polymer is commercially distributed by Flintbox (flintbox.com/public/project/1948/).

Immunoflourescence

Podocytes grown on coverslips (50% confluency) were washed with 1x PBS, fixed using 4% PFA at room temperature for 10 min and immunostaining was performed as described previously . Samples were blocked using 5% donkey serum dissolved in 0.1% Triton in PBS. Antibodies were used in a 1:400 dilution in PBS for overnight incubation. Next, slides were washed using PBS for three times and were decorated with phalloidin (1:100) coupled to Cy5 and a Cy3 or Alexa 488 labeled secondary antibody (Jackson ImmunoResearch). Samples were washed with PBS and DAPI and samples were mounted using Prolong Gold (Thermo Scientific).

Rats, PAN treatment and glomerular isolation.

Rats were housed in a specific pathogen–free facility with free access to chow and water and a 12-hour day/12-hour night cycle. Animal procedures were approved by local authorities (Regierungspräsidium Freiburg G15-134). Male CD IGS rats [Crl:CD(SD)] (body weight, 101 to 125 g) were obtained from Charles River. Animals were randomly assigned to treatment groups. Animals were treated by intraperitoneal injection of either PAN (15 mg/100 g body weight) (Santa Cruz Biotechnology) dissolved in 0.9% NaCl or solvent alone (26). Kidneys were removed in deep anesthesia [ketamine (100 mg/kg) and xylazine (5 mg/kg) in 0.9% NaCl (10 µl/g)] and immediately perfused with ice-cold Hanks' balanced salt solution (HBSS) via the renal arteries. The renal cortex was removed and minced, and the glomeruli were isolated using the sieving method, which results in 95% purity of glomeruli in the preparation. The following sieve sizes were used: 180, 106, and 53 µm. The tissues were constantly rinsed with 4°C cold HBSS during glomeruli isolation. The glomeruli

were collected on the lowest sieve. Purity of renal glomeruli was verified using light microscopy. The final glomerular pellet was obtained by centrifugation at 2300 rpm for 7 min and was snap-frozen in liquid nitrogen.

The rats used for immunoblotting were phenotyped for proteinuria in the previous study [44], and an untouched aliquot of glomeruli were used. At day 2, rats were sacrificed and glomeruli fractions were obtained by sieving of the perfused kidneys. An aliquot of glomeruli was snap-frozen and stored at -80 degrees. Then, glomeruli were lysed in 4% SDS, and lysates were sonicated, boiled and subjected to immunoblotting as described above. No further freeze-thaw cycles were introduced. The rats used for degradomic studies were sacrificed at day 4 and glomeruli were lysed and processed as described in the "proteome preparation" and "TAILS" section.

WT1 knockout mouse model.

Male proteinuric WT1 heterozygous mice (FVB background) in the age of 14 weeks were compared to wildtype male control animals (littermates). Proteinuria was validated by gel electrophoresis and coomassie staining. The mouse model was previously described [45]. Glomerular preparation was performed as described above. Glomeruli were lysed in 4% SDS buffer and the subjected to immunoblotting as described above. The experimental protocol was examined and approved by the LANUV NRW (Landesamt für Natur, Umwelt und Verbraucherschutz Nordrhein-Westfalen/State Agency for Nature, Environment and Consumer Protection North Rhine-Westphalia).

Primary Antibodies

Protein	Company	species	Application	Dilution	Cat No	Epitope
Vimentin	Cell signaling	rabbit polyclonal antibody	Western Blot IF	1:1000 1:1000	#5741	Oligopeptide Surrounding Arg 45
Vimentin	Santa Cruz	goat polyclonal antibody	western Blot	1: 1000	sc-7558	Oligopeptide at the C terminus
ACTN4 (cross reactivity ACTN1)	BD	mouse monoclonal antibody	Western Blot	1:1000	612576	AA 629-825

Podocin	Sigma	mouse monoclonal antibody	Western Blot	1:1000	P0372	AA 367-383
Podocin	Santa cruz	rabbit polyclonal AB	Western Blot	1:1000	sc-21009	AA 1-130.
Filamin	Cell signaling	Rabbit polyclonal AB	Western Blot	1:1000	#4762	unknown
Myh9	Sigma	Rabbit polyclonal antibody	Western Blot	1:1000	M8064	AA 1949-1960

Secondary antibodies and other dyes.

Antibody	**Company**	**Cat. No.**	**Application**	**Dilution**
Rabbit anti-goat, HRP coupled	Dako	E046601-2	Immunoblot, ECL	1:25000
Donkey anti rabbit, IRDye ® 680RD	Licor	926-68073	Immunoblot, Licor	1:25000
Donkey anti mouse 800 IRDye ® 800 RD	Licor	926-32280	Immunoblot, Licor	1:25000
Donkey anti rabbit, A488	Jackson ImmunoResearch	711-546-152	Immunofluorescence	1:400
Donkey anti mouse Cy 3	Jackson ImmunoResearch	715-165-150	Immunofluorescence	1:400
Donkey anti mouse A488	Jackson ImmunoResearch	715-545-150	Immunofluorescence	1:400
Phalloidin, 647	Dyomics	647P1-33	Immunofluorescence	1:400
Dapi	Invitrogen	D1306	Immunofluorescence	1:10000

Acknowledgement

This work was supported by the DFG (UoC PostDoc grant to M.M.R; CRC 1140 KIDGEM to FG and TBH, CRC 992 and HU 1016/8-1 to TBH and an intramural Koeln-Fortune Grant (to M.M.R.). TBH was supported by the BMBF (01GM1518C), by the European Research Council (ERC grant 616891 and H2020-IMI2 consortium BEAt-DKD) and by the Excellence Initiative of the German Federal and State Governments (BIOSS). The lab of P.F.H. is in part supported by an ERC starting grant (ID 639905). The authors acknowledge excellent technical support by Ruth Herzog (Cologne), Astrid Wilbrand-Hennes (Cologne) and Nadine Wettengl (Juelich). The authors acknowledge the CECAD proteomics core facility. JNK is the recipient of a Career Investigator Scholar award from Michael Smith Foundation of Health Research. JNK acknowledges the funding from Natural Science and Engineering Research Council (NSERC) of Canada. The author contributions were as follows: Designed study: MMR, PFH, TB. Wrote Paper: MMR, PFH, TB. Performed experiments: MMR, AKH, FG, JB, LAV, ES, MH, MM. Analyzed Data: MMR, PFH, TB. Interpreted data: MMR; PFH; BS, TB. Contributed new tools: CK, JNK, MK, TBH

.

Statement of competing financial interests

The authors have nothing to disclose and no competing financial interests regarding this project.

References

1. Pavenstädt H, Kriz W, Kretzler M: Cell biology of the glomerular podocyte. *Physiol. Rev.* 83: 253–307, 2003

2. Brinkkoetter PT, Ising C, Benzing T: The role of the podocyte in albumin filtration. *Nat. Rev. Nephrol.* 9: 328–336, 2013

3. Boute N, Gribouval O, Roselli S, Benessy F, Lee H, Fuchshuber A, Dahan K, Gubler MC, Niaudet P, Antignac C: NPHS2, encoding the glomerular protein podocin, is mutated in autosomal recessive steroid-resistant nephrotic syndrome. *Nat. Genet.* 24: 349–354, 2000

4. Kestilä M, Lenkkeri U, Männikkö M, Lamerdin J, McCready P, Putaala H, Ruotsalainen V, Morita T, Nissinen M, Herva R, Kashtan CE, Peltonen L, Holmberg C, Olsen A, Tryggvason K: Positionally cloned gene for a novel glomerular protein--nephrin--is mutated in congenital nephrotic syndrome. *Mol. Cell* 1: 575–582, 1998

5. Kaplan JM, Kim SH, North KN, Rennke H, Correia LA, Tong HQ, Mathis BJ, Rodríguez-Pérez JC, Allen PG, Beggs AH, Pollak MR: Mutations in ACTN4, encoding alpha-actinin-4, cause familial focal segmental glomerulosclerosis. *Nat. Genet.* 24: 251–256, 2000

6. Lange PF, Overall CM: Protein TAILS: when termini tell tales of proteolysis and function. *Curr. Opin. Chem. Biol.* 17: 73–82, 2013

7. Vandenbroucke RE, Libert C: Is there new hope for therapeutic matrix metalloproteinase inhibition? *Nat. Rev. Drug Discov.* 13: 904–927, 2014

8. Kistler AD, Peev V, Forst A-L, El Hindi S, Altintas MM, Reiser J: Enzymatic disease of the podocyte. *Pediatr. Nephrol. Berl. Ger.* 25: 1017–1023, 2010

9. Yaddanapudi S, Altintas MM, Kistler AD, Fernandez I, Möller CC, Wei C, Peev V, Flesche JB, Forst A-L, Li J, Patrakka J, Xiao Z, Grahammer F, Schiffer M, Lohmüller T, Reinheckel T, Gu C, Huber TB, Ju W, Bitzer M, Rastaldi MP, Ruiz P, Tryggvason K, Shaw AS, Faul C, Sever S, Reiser J: CD2AP in mouse and human podocytes controls a proteolytic program that regulates cytoskeletal structure and cellular survival. *J. Clin. Invest.* 121: 3965–3980, 2011

10. Yamamoto-Nonaka K, Koike M, Asanuma K, Takagi M, Trejo JAO, Seki T, Hidaka T, Ichimura K, Sakai T, Tada N, Ueno T, Uchiyama Y, Tomino Y: Cathepsin D in Podocytes Is Important in the Pathogenesis of Proteinuria and CKD. *J. Am. Soc. Nephrol.* ASN.2015040366, 2016

11. Li S-Y, Huang P-H, Yang A-H, Tarng D-C, Yang W-C, Lin C-C, Chen J-W, Schmid-Schönbein G, Lin S-J: Matrix metalloproteinase-9 deficiency attenuates diabetic nephropathy by modulation of podocyte functions and dedifferentiation. *Kidney Int.* 86: 358–369, 2014

12. Rinschen MM, Schroeter CB, Koehler S, Ising C, Schermer B, Kann M, Benzing T, Brinkkoetter PT: Quantitative deep-mapping of the cultured podocyte

proteome uncovers shifts in proteostatic mechanisms during differentiation. *Am. J. Physiol. Cell Physiol.* ajpcell.00121.2016, 2016

13. Altintas MM, Moriwaki K, Wei C, Möller CC, Flesche J, Li J, Yaddanapudi S, Faridi MH, Gödel M, Huber TB, Preston RA, Jiang JX, Kerjaschki D, Sever S, Reiser J: Reduction of proteinuria through podocyte alkalinization. *J. Biol. Chem.* 289: 17454–17467, 2014

14. Sever S, Altintas MM, Nankoe SR, Möller CC, Ko D, Wei C, Henderson J, del Re EC, Hsing L, Erickson A, Cohen CD, Kretzler M, Kerjaschki D, Rudensky A, Nikolic B, Reiser J: Proteolytic processing of dynamin by cytoplasmic cathepsin L is a mechanism for proteinuric kidney disease. *J. Clin. Invest.* 117: 2095–2104, 2007

15. Lai ZW, Petrera A, Schilling O: Protein amino-terminal modifications and proteomic approaches for N-terminal profiling. *Curr. Opin. Chem. Biol.* 24: 71–79, 2015

16. Huesgen PF, Lange PF, Rogers LD, Solis N, Eckhard U, Kleifeld O, Goulas T, Gomis-Rüth FX, Overall CM: LysargiNase mirrors trypsin for protein C-terminal and methylation-site identification. *Nat. Methods* 12: 55–58, 2015

17. Huesgen PF, Lange PF, Overall CM: Ensembles of protein termini and specific proteolytic signatures as candidate biomarkers of disease. *Proteomics Clin. Appl.* 8: 338–350, 2014

18. Kleifeld O, Doucet A, auf dem Keller U, Prudova A, Schilling O, Kainthan RK, Starr AE, Foster LJ, Kizhakkedathu JN, Overall CM: Isotopic labeling of terminal amines in complex samples identifies protein N-termini and protease cleavage products. *Nat. Biotechnol.* 28: 281–288, 2010

19. Völker LA, Schurek E-M, Rinschen MM, Tax J, Schutte BA, Lamkemeyer T, Ungrue D, Schermer B, Benzing T, Höhne M: Characterization of a short isoform of the kidney protein podocin in human kidney. *BMC Nephrol.* 14: 102, 2013

20. Weber S, Gribouval O, Esquivel EL, Morinière V, Tête M-J, Legendre C, Niaudet P, Antignac C: NPHS2 mutation analysis shows genetic heterogeneity of steroid-resistant nephrotic syndrome and low post-transplant recurrence. *Kidney Int.* 66: 571–579, 2004

21. Shankland SJ: The podocyte's response to injury: role in proteinuria and glomerulosclerosis. *Kidney Int.* 69: 2131–2147, 2006

22. Kanjanabuch T, Ma L-J, Chen J, Pozzi A, Guan Y, Mundel P, Fogo AB: PPAR-gamma agonist protects podocytes from injury. *Kidney Int.* 71: 1232–1239, 2007

23. Lee HW, Khan SQ, Faridi MH, Wei C, Tardi NJ, Altintas MM, Elshabrawy HA, Mangos S, Quick KL, Sever S, Reiser J, Gupta V: A Podocyte-Based Automated Screening Assay Identifies Protective Small Molecules. *J. Am. Soc. Nephrol. JASN* 26: 2741–2752, 2015

24. Colaert N, Helsens K, Martens L, Vandekerckhove J, Gevaert K: Improved visualization of protein consensus sequences by iceLogo. *Nat. Methods* 6: 786–787, 2009

25. Sanwal V, Pandya M, Bhaskaran M, Franki N, Reddy K, Ding G, Kapasi A, Valderrama E, Singhal PC: Puromycin aminonucleoside induces glomerular epithelial cell apoptosis. *Exp. Mol. Pathol.* 70: 54–64, 2001

26. Fortelny N, Cox JH, Kappelhoff R, Starr AE, Lange PF, Pavlidis P, Overall CM: Network analyses reveal pervasive functional regulation between proteases in the human protease web. *PLoS Biol.* 12: e1001869, 2014

27. Rinschen MM, Wu X, König T, Pisitkun T, Hagmann H, Pahmeyer C, Lamkemeyer T, Kohli P, Schnell N, Schermer B, Dryer S, Brooks BR, Beltrao P, Krueger M, Brinkkoetter PT, Benzing T: Phosphoproteomic Analysis Reveals Regulatory Mechanisms at the Kidney Filtration Barrier. *J. Am. Soc. Nephrol. JASN* 2014

28. Hoffert JD, Pisitkun T, Knepper MA: Phosphoproteomics of vasopressin signaling in the kidney. *Expert Rev. Proteomics* 8: 157–163, 2011

29. Rinschen MM, Benzing T, Limbutara K, Pisitkun T: Proteomic analysis of the kidney filtration barrier - problems and perspectives. *Proteomics Clin. Appl.* 2015

30. Rinschen MM, Pahmeyer C, Pisitkun T, Schnell N, Wu X, Maaß M, Bartram MP, Lamkemeyer T, Schermer B, Benzing T, Brinkkoetter PT: Comparative phosphoproteomic analysis of mammalian glomeruli reveals conserved podocin C-terminal phosphorylation as a determinant of slit diaphragm complex architecture. *Proteomics* 15: 1326–1331, 2015

31. Rinschen MM, Schermer B, Benzing T: Vasopressin-2 receptor signaling and autosomal dominant polycystic kidney disease: from bench to bedside and back again. *J. Am. Soc. Nephrol. JASN* 25: 1140–1147, 2014

32. Talbot JJ, Song X, Wang X, Rinschen MM, Doerr N, LaRiviere WB, Schermer B, Pei YP, Torres VE, Weimbs T: The cleaved cytoplasmic tail of polycystin-1 regulates Src-dependent STAT3 activation. *J. Am. Soc. Nephrol. JASN* 25: 1737–1748, 2014

33. Bartram MP, Habbig S, Pahmeyer C, Höhne M, Weber LT, Thiele H, Altmüller J, Kottoor N, Wenzel A, Krueger M, Schermer B, Benzing T, Rinschen MM, Beck BB: Three-layered proteomic characterization of a novel ACTN4 mutation unravels its pathogenic potential in FSGS. *Hum. Mol. Genet.* 2016

34. Rinschen MM, Schroeter CB, Koehler S, Ising C, Schermer B, Kann M, Benzing T, Brinkkoetter PT: Quantitative deep mapping of the cultured podocyte proteome uncovers shifts in proteostatic mechanisms during differentiation. *Am. J. Physiol. Cell Physiol.* 311: C404-417, 2016

35. Saleem MA, O'Hare MJ, Reiser J, Coward RJ, Inward CD, Farren T, Xing CY, Ni L, Mathieson PW, Mundel P: A conditionally immortalized human podocyte cell line demonstrating nephrin and podocin expression. *J. Am. Soc. Nephrol. JASN* 13: 630–638, 2002

36. Boersema PJ, Raijmakers R, Lemeer S, Mohammed S, Heck AJR: Multiplex peptide stable isotope dimethyl labeling for quantitative proteomics. *Nat. Protoc.* 4: 484–494, 2009

37. Rappsilber J, Ishihama Y, Mann M: Stop and go extraction tips for matrix-assisted laser desorption/ionization, nanoelectrospray, and LC/MS sample pretreatment in proteomics. *Anal. Chem.* 75: 663–670, 2003

38. Rinschen MM, Bharill P, Wu X, Kohli P, Reinert MJ, Kretz O, Martinez IS, Schermer B, Höhne M, Bartram MP, Aravamudhan S, Brooks BR, Vilchez D, Huber TB, Müller R-U, Krüger M, Benzing T: The ubiquitin ligase Ubr4 controls stability of podocin/MEC-2 supercomplexes. *Hum. Mol. Genet.* 2016

39. Beck S, Michalski A, Raether O, Lubeck M, Kaspar S, Goedecke N, Baessmann C, Hornburg D, Meier F, Paron I, Kulak NA, Cox J, Mann M: The Impact II, a Very High-Resolution Quadrupole Time-of-Flight Instrument (QTOF) for Deep Shotgun Proteomics. *Mol. Cell. Proteomics MCP* 14: 2014–2029, 2015

40. Cox J, Mann M: MaxQuant enables high peptide identification rates, individualized p.p.b.-range mass accuracies and proteome-wide protein quantification. *Nat. Biotechnol.* 26: 1367–1372, 2008

41. Fortelny N, Yang S, Pavlidis P, Lange PF, Overall CM: Proteome TopFIND 3.0 with TopFINDer and PathFINDer: database and analysis tools for the association of protein termini to pre- and post-translational events. *Nucleic Acids Res.* 43: D290-297, 2015

42. Tyanova S, Temu T, Sinitcyn P, Carlson A, Hein MY, Geiger T, Mann M, Cox J: The Perseus computational platform for comprehensive analysis of (prote)omics data. *Nat. Methods* 13: 731–740, 2016

43. Zhao B, Pisitkun T, Hoffert JD, Knepper MA, Saeed F: CPhos: a program to calculate and visualize evolutionarily conserved functional phosphorylation sites. *Proteomics* 12: 3299–3303, 2012

44. Rinschen MM, Grahammer F, Hoppe A-K, Kohli P, Hagmann H, Kretz O, Bertsch S, Höhne M, Göbel H, Bartram MP, Gandhirajan RK, Krüger M, Brinkkoetter P-T, Huber TB, Kann M, Wickström SA, Benzing T, Schermer B: YAP-mediated mechanotransduction determines the podocyte's response to damage. *Sci. Signal.* 10: 2017

45. Schumacher VA, Schlötzer-Schrehardt U, Karumanchi SA, Shi X, Zaia J, Jeruschke S, Zhang D, Pavenstädt H, Pavenstaedt H, Drenckhan A, Amann K, Ng C, Hartwig S, Ng K-H, Ho J, Kreidberg JA, Taglienti M, Royer-Pokora B, Ai X: WT1-dependent sulfatase expression maintains the normal glomerular filtration barrier. *J. Am. Soc. Nephrol. JASN* 22: 1286–1296, 2011

46. Büscher AK, Kranz B, Büscher R, Hildebrandt F, Dworniczak B, Pennekamp P, Kuwertz-Bröking E, Wingen A-M, John U, Kemper M, Monnens L, Hoyer PF, Weber S, Konrad M: Immunosuppression and renal outcome in congenital and pediatric steroid-resistant nephrotic syndrome. *Clin. J. Am. Soc. Nephrol. CJASN* 5: 2075–2084, 2010

47. Schoeb DS, Chernin G, Heeringa SF, Matejas V, Held S, Vega-Warner V, Bockenhauer D, Vlangos CN, Moorani KN, Neuhaus TJ, Kari JA, MacDonald J, Saisawat P, Ashraf S, Ovunc B, Zenker M, Hildebrandt F, Gesselschaft für Paediatrische Nephrologie (GPN) Study Group: Nineteen novel NPHS1 mutations in a worldwide cohort of patients with congenital nephrotic syndrome (CNS). *Nephrol. Dial. Transplant. Off. Publ. Eur. Dial. Transpl. Assoc. - Eur. Ren. Assoc.* 25: 2970–2976, 2010

48. Philippe A, Nevo F, Esquivel EL, Reklaityte D, Gribouval O, Tête M-J, Loirat C, Dantal J, Fischbach M, Pouteil-Noble C, Decramer S, Hoehne M, Benzing T, Charbit M, Niaudet P, Antignac C: Nephrin mutations can cause childhood-onset steroid-resistant nephrotic syndrome. *J. Am. Soc. Nephrol. JASN* 19: 1871–1878, 2008

49. Machuca E, Benoit G, Nevo F, Tête M-J, Gribouval O, Pawtowski A, Brandström P, Loirat C, Niaudet P, Gubler M-C, Antignac C: Genotype-phenotype correlations in non-Finnish congenital nephrotic syndrome. *J. Am. Soc. Nephrol. JASN* 21: 1209–1217, 2010

50. Choi HJ, Lee BH, Cho HY, Moon KC, Ha IS, Nagata M, Choi Y, Cheong HI: Familial focal segmental glomerulosclerosis associated with an ACTN4 mutation and paternal germline mosaicism. *Am. J. Kidney Dis. Off. J. Natl. Kidney Found.* 51: 834–838, 2008

Figure Legends

Figure 1. Identification of processed proteoforms in mouse glomeruli by N degradomics.
A. Scheme of the TAILS workflow (see main text and methods for details).
B. Classification of protein N-termini identified by TAILS-experiments (see methods for details). Expected termini are distinguished in termini with intact (P1) or removed (P2) initiating Met mapping to the start of the longest known isoform, termini starting at annotated signal peptide cleavage sites, previously identified protease-generated N-termini and termini explained by alternative splicing sites. Unexpected N-termini are neither annotated nor observed previously and occurred either within or outside annotated protein domains. Blue, dimethylated termini modified in vivo representing protease-generated neo-N-termini by proteolytic cleavage); black, acetylated termini modified endogenously; red, termini found in both acetylated and dimethylated forms (Stably endogenous) are distinguished.
C. Known cleavage sites as annotated by the TOPFINDer algorithm. Cathepsins (CATE,CATD) were the most abundant cleavage sites in glomeruli. Cleavage sites of CATD were statistically overrepresented in the dataset as compared to the previously published terminome (cyan color, Bonferroni corrected Fishers exact test, $p<0.05$).
D. Immunoblot for podocin from isolated glomeruli (left) and snap-frozen mouse kidney using two antibodies against two different epitopes. (*) denotes a band at 34 kDa.
E. Immunoblot of mouse and human glomerular proteins for podocin detects a conserved lower molecular weight band (*).
F. Overview of novel cleavage sites on nephrin (NPHS1), podocin (NPHS2) and ACTN4 and their vicinity to known point mutations causing hereditary nephrotic syndrome and/or FSGS. The mutations are as follows: NPHS1: Leu96Val, Asp105Asn, Ala107Thr , Ala107Glu, Ala107Val [46–48] and Arg299Pro, Arg299Cys, Asp310Asn [47,49]. NPHS2: A61V (a polymorphism with yet unknown pathogenicity [20]), ACTN4: Lys255Glu, Thr259Ile, Ser262Pro, Ser262Phe [5,50]. Mutations are depicted in red, and polymorphism in magenta, and the most adjacent neo-termini peptide is depicted in yellow. All detected cleavage sites are depicted as black arrows.

Figure 2. Quantitative protein N termini profiling in cultured podocytes
A. Positional classification of N-termini in cultured podocytes.
B. Quantile analysis of quantified neo N-termini (n=666). The log2 ratio (PAN/vehicle) is plotted against the log2 rank. Termini reproducibly quantified in the first (decreased, first quantile, green) and last quantile (increased, 10th quantile, magenta) were further analysed.
C. Gene ontology analysis of N-termini increased and decreased by PAN. GO-BP Slim terms significantly overrepresented (Fishers exact test, $p<0.01$ and FDR <0.01) are depicted in the bar graph. The enrichment factor vs the unchanged protein population is indicated at the X-axis..
D. Cumulative histogram of actin binding proteins and all other proteins. On a global level, the distribution of ratios of actin-binding proteins was different as compared to the other proteins (Kolmogorov-Smirnoff-Test $p<0.001$).
E. Overview of ACTN4 cleavage sites. The X axis denotes the residue number of the protein, and the Y axis the log2 fold change of PAN/veh treatment. Each terminus is denoted with its regulation. The colour background denotes cutoffs for increased (magenta) and decreased (green) termini. In ACTN4 protein, 5 termini were

identified by TAILSs. Of these, two were significantly regulated. An antibody with a C-terminal epitope (indicated) detected 5 of the resulting proteoforms. All of the regulated sites were conserved in mouse glomeruli.
F. ACTN4 proteoforms visualized by immunoblotting as low-molecular weight bands. Quantification of intensity of the proteoform bands (P2-5) over full-length protein (P0) by densitometry demonstrated significant regulation of proteolytic processing during PAN injury, consistent with the TAILS data. * = $p < 0.05$ in a two-tailed t-test.

Figure 3 Protease class analysis reveals caspase 3/6 activation as an overarching signaling mechanism in PAN injury.
A. Position weighted matrix of Neo-termini in the decreased termini population. The one letter code demonstrates the frequency of each amino acid as compared to the unchanged termini population. The arrow indicates the cleavage site of the protease. The motif of proteases cleaving after an Arginine, “R”, is overrepresented in the decreased termini population (as compared to non-changed termini). This matrix corresponds to a Serine protease motif.
B. Position weighted matrix of Neo-termini in the increased termini population. The arrow indicates the cleavage site of the protease. The motif of proteases cleaving after an Aspartate, “D”, is overrepresented in the decreased termini population. This motif corresponds to a caspase motif.
C. Immunoblot for cleaved caspase 3-6 (Asp175). Protein lysates of human podocytes treated with PAN (50 µg/mL) for the indicated time points. Immunoblots were stained with a cleaved-caspase specific antibody, beta tubulin indicated a loading control. * delineates significance in a two-way ANOVA with Dunetts post-test vs veh (0h PAN treatment), $p<0.05$, n=5.
D. Protease web [26] of activated caspase 3 in the dataset. Dark circles correspond to hits from the dataset. The protease of interest (caspase 3) is connected with downstream substrates inherent to this dataset. Caspase activates a variety of other proteases, including caspase 6, 7,8 and the mitochondrial proteases PMPCB2, MTAP2 and cathepsin B. Substrates include mainly structural and metabolic targets of caspases, as well as the intermediate filament protein vimentin (D85).
E. Overview of Vimentin cleavage sites. The X axis denotes the residue number of the protein, and the Y axis the log2 fold change of PAN/veh treatment. Each terminus is depicted with its regulation. The colour background denotes statistical cutoffs for increased (magenta) and decreased (green) termini. In the vimentin protein, many cleavages can be found by TAILS analysis. One of the increased cleavage sites (D85) is a known caspase cleavage site. All of the regulated sites are also present in native mouse glomeruli.
F. Immunoblot of PAN treated podocytes for Vimentin. Two of the detected proteoforms (P1,2) can be visualized by immunoblot using specific antibodies with defined epitopes. Quantification of intensity of the proteoform bands (P1+2) over full length protein (P0) was performed using densitometry. * = $p < 0.05$ in a two-tailed t-test.

Figure 4 Proteolytic events are partially conserved in *in vivo* podocyte injury models.
A. Classification of protein N-termini identified by TAILS-experiments in PAN treated rats. A binary decision tree was used to classify proteins. A majority of proteolytic N-termini (indicated by dimethylated termini) localizes to extracellular compartments.
B. Structure of vimentin and localization of a proteolytic cleavage site determined in mouse glomeruli, human podocyte cells, and rat glomeruli. The cleavage ocurrs

between residue R196 and E197 in all three species. The cleavage process is reduced and in the top regulated quantile in both PAN injury models.
C. Immunoblot of lysates from isolated glomeruli of rats treated with PAN for two days vs vehicle control. Immunoblot was probed for vimentin using an N-temrinal antibody. One cleaved proteoform can be visualized by the antibody in both human cells and rat glomeruli. Quantification of intensity of the cleaved proteoform bands (Pcl) over full length protein (P0) was performed using densitometry (only for rat glomeruli, n= 3). * = $p < 0.05$ in a two-tailed t-test.
D. Immunoblot of glomeruli of rats treated with PAN for two days vs vehicle control. Immunoblot was probed for alpha-actinin. Several cleaved proteoforms (Pcl) can be visualized by immunoblot using specific antibodies. Quantification of intensity of the cleaved proteoform bands (Pcl) over full length protein (P0) was performed using densitometry (only for rat glomeruli, n=3). * = $p < 0.05$ in a two-tailed t-test.
E. Immunoblot of glomeruli from WT1 heterozygous knockout mice (WT1KO/WT) and control (wildtype) littermates. Immunoblot was probed for alpha-actinin. Quantification of intensity of the cleaved proteoform bands (Pcl) over full length protein (P0) was performed using densitometry. * = $p < 0.05$ in a two-tailed t-test.

Tables

Table 1: Selected Neo-termini of important podocyte proteins.

Gene symbol	Protein (Uniprot)	Sequence of terminus found in glomerulus *	MQ score	Residue	Cleavage site annotation	Homologous terminus in human cultured podocyte **
Nphs2	Podocin (Q91X05)	APAATATVVDVDEVR AATATVVDVDEVR ATATVVDVDEVR TATVVDVDEVR ATVVDVDEVR TVVDVDEVR	103.88 99,94 78,96 94,77 150,04 82,01	A59 A61 A62 T63 A64 T65	Unexpected Unexpected Unexpected Unexpected Unexpected Unexpected	N/A N/A N/A N/A N/A N/A
Nphs1	Nephrin (Q9QZS7)	IEACDLSDDAEYECQVGR VMTVRPEDHGAR	160.55 55.04	I112 V317	Unexpecte, Extracellular	N/A N/A
Kirrel	Neph1 (Q80W68)	TRFSQEPADQTVVAGQR	137.91	T53	Signal peptide	Yes, T21
Actn4	Actinin-4 (P57780)	TQIENIDEDFR	170.95	T69	Unexpected	Yes, T70
Podxl	Podocalyxin (Q9R0M4)	HVAPILDNQAVAVKR VAPILDNQAVAVKR	77.78 89.23	H343 V344	Unexpected Unexpected	N/A N/A
Myh9	Myosin IIa (Q8VDD5)	TQISELQEDLESER TLDSTAAQQELR TQELLQEENR	93.42 71.59 66.02	T1111 T1151 T1313	Unexpected Unexpected Unexpected	Yes,S1111 Yes,T1151 Yes, T1313
Arhgdia	Arhgdia (Q99PT1)	SIQEIQELDKDDESLR	54.00	S34	Unexpected	Yes, S34
Itgb1	Integrin beta-1 (P09055)	TDEVNSEDMDAYCR	124.25	T504	extracellular	Yes, T504
Calm	Calmodulin (P62204)	DKDGDGTITTKELGTVMR	82.01	D21	Cathepsin D/E cleavage	Yes, F20 ***

(*) All N-termini are Dimethyllabeled. For more mass spectrometric details, please see supplemental datasets, or deposited raw data (see method for accessions).

(**)Homologous, conserved cleavage sites were determined by the CPHOS software [43].

(***) In the human podocytes, this terminus occurs one amino acid N-terminal of the homologous amino acid.

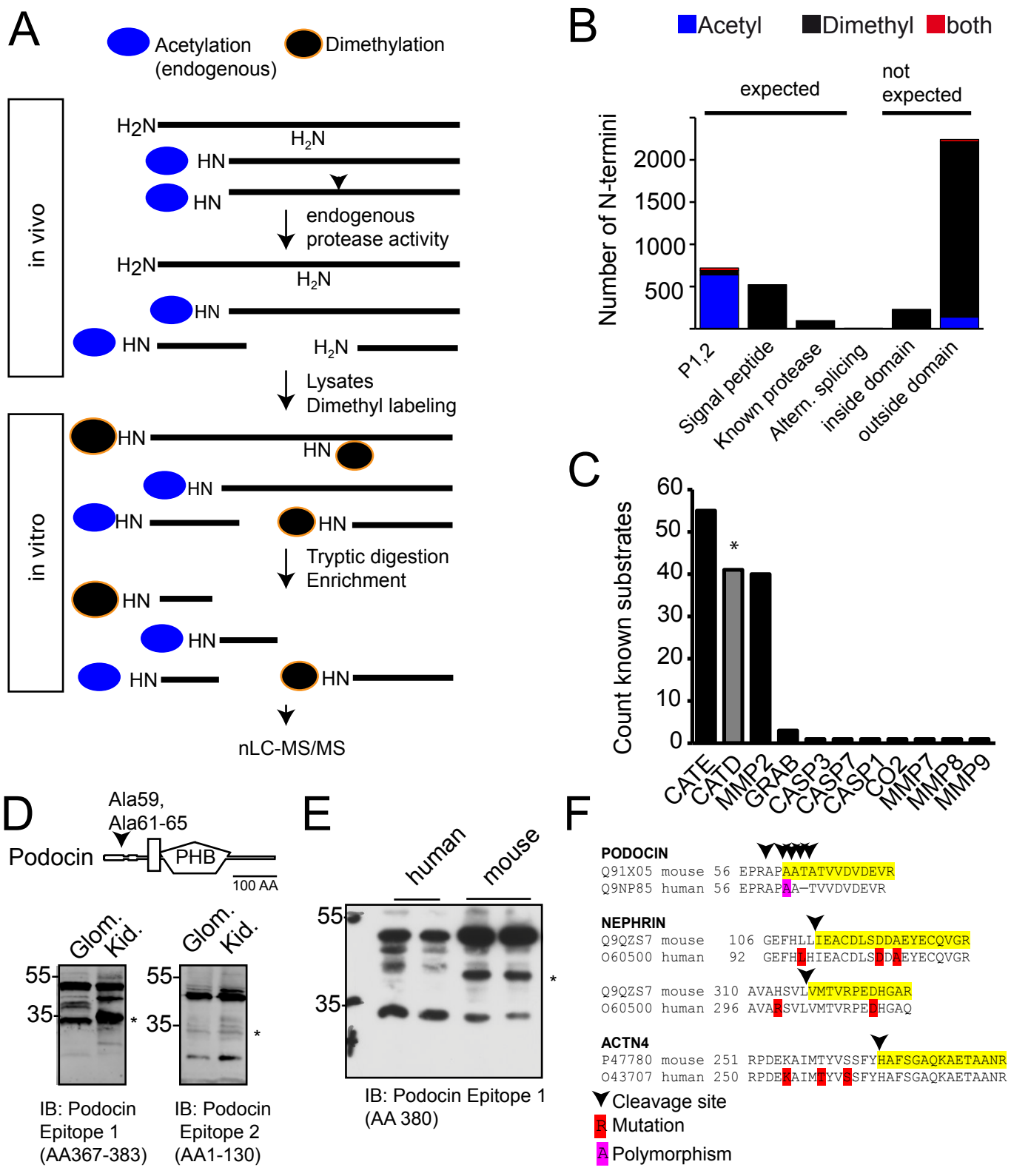
A
Acetylation (endogenous)
Dimethylation
in vivo
in vitro
endogenous protease activity
Lysates Dimethyl labeling
Tryptic digestion Enrichment
nLC-MS/MS
B
Acetyl
Dimethyl
both
expected
not expected
Number of N-termini
2000
1500
1000
500
P1,2
Signal peptide
Known protease
Altern. splicing
inside domain
outside domain
C
Count known substrates
60
50
40
30
20
10
0
CATE
CATD
MMP2
GRAB
CASP3
CASP7
CASP1
CO2
MMP7
MMP8
MMP9
D
Ala59, Ala61-65
Podocin
PHB
100 AA
Glom.
Kid.
55
35
IB: Podocin Epitope 1 (AA367-383)
IB: Podocin Epitope 2 (AA1-130)
E
human
mouse
55
35
IB: Podocin Epitope 1 (AA 380)
F
PODOCIN
Q91X05 mouse 56 EPRAPAATATVVDVDEVR
Q9NP85 human 56 EPRAPAA–TVVDVDEVR
NEPHRIN
Q9QZS7 mouse 106 GEFHLLIEACDLSDDAEYECQVGR
O60500 human 92 GEFHLHIEACDLSDDAEYECQVGR
Q9QZS7 mouse 310 AVAHSVLVMTVRPEDHGAR
O60500 human 296 AVARSVLVMTVRPEDHGAQ
ACTN4
P47780 mouse 251 RPDEKAIMTYVSSFYHAFSGAQKAETAANR
O43707 human 250 RPDEKAIMTYVSSFYHAFSGAQKAETAANR
Cleavage site
R Mutation
A Polymorphism

Fig. 1

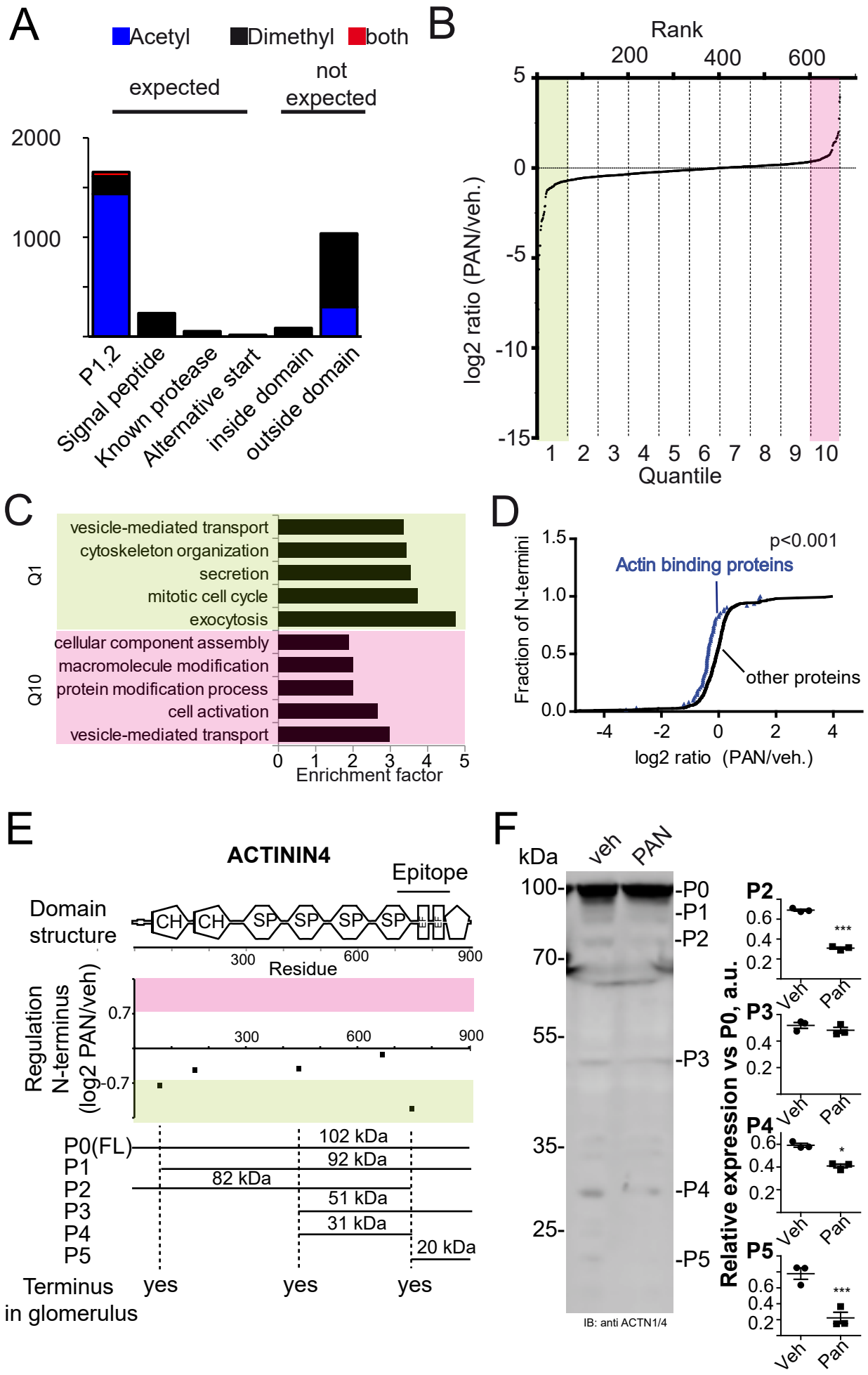
A
Acetyl
Dimethyl
both
expected
not expected
2000
1000
P1,2
Signal peptide
Known protease
Alternative start
inside domain
outside domain
B
Rank
200
400
600
5
0
-5
-10
-15
log2 ratio (PAN/veh.)
1 2 3 4 5 6 7 8 9 10
Quantile
C
Q1
vesicle-mediated transport
cytoskeleton organization
secretion
mitotic cell cycle
exocytosis
Q10
cellular component assembly
macromolecule modification
protein modification process
cell activation
vesicle-mediated transport
0 1 2 3 4 5
Enrichment factor
D
p<0.001
Actin binding proteins
other proteins
Fraction of N-termini
1.5
1.0
0.5
0.0
-4 -2 0 2 4
log2 ratio (PAN/veh.)
E
ACTININ4
Epitope
Domain structure
CH CH SP SP SP SP EF EF
300 600 900
Residue
Regulation N-terminus (log2 PAN/veh)
0.7
-0.7
300 600 900
P0(FL)
P1
P2
P3
P4
P5
102 kDa
92 kDa
82 kDa
51 kDa
31 kDa
20 kDa
Terminus in glomerulus
yes
yes
yes
F
kDa
veh
PAN
100-
70-
55-
35-
25-
-P0
-P1
-P2
-P3
-P4
-P5
IB: anti ACTN1/4
Relative expression vs P0, a.u.
P2
P3
P4
P5
0.6
0.4
0.2
***
*
Veh
Pan

Fig. 2

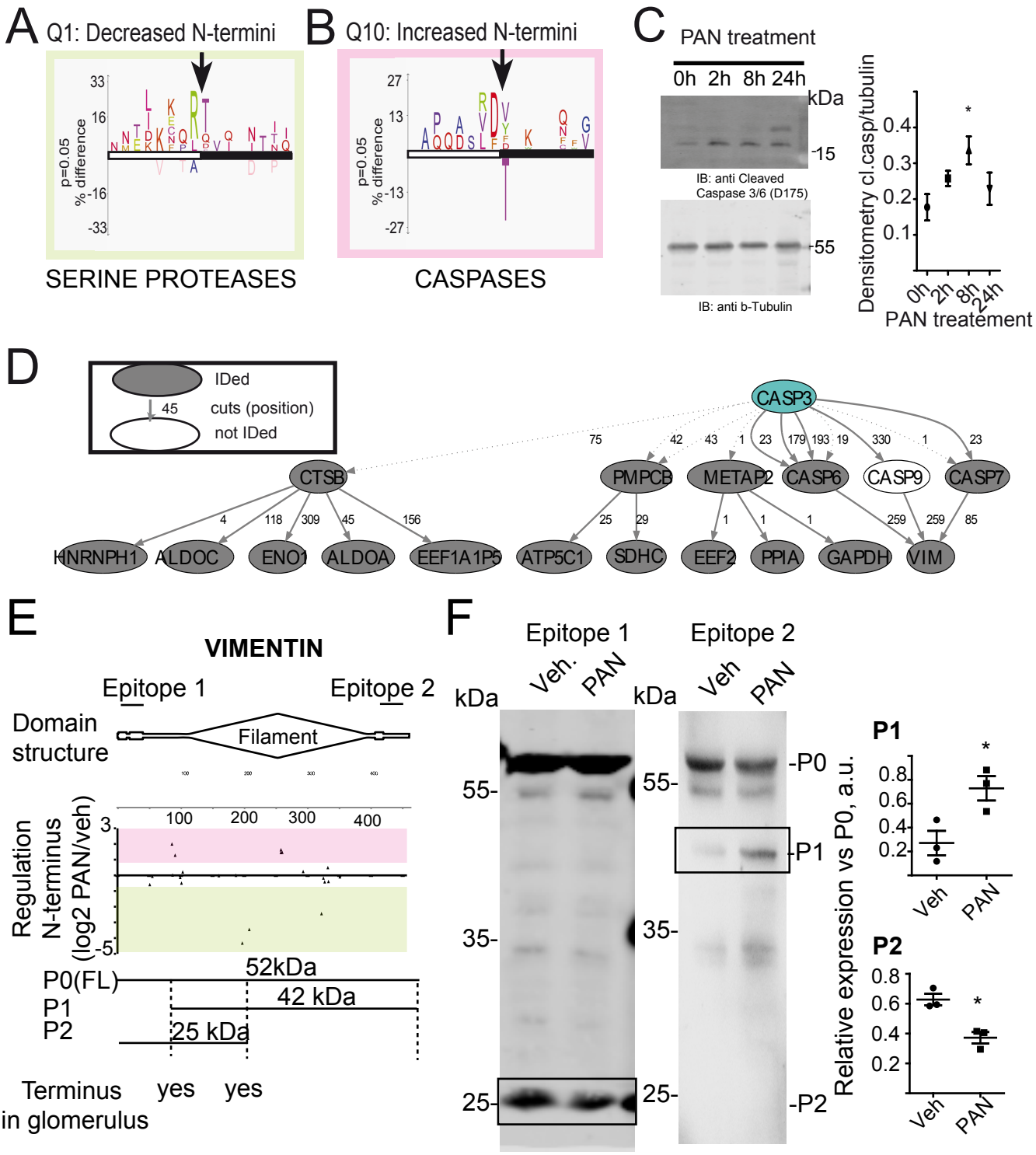
A
Q1: Decreased N-termini
p=0.05
% difference
SERINE PROTEASES
B
Q10: Increased N-termini
CASPASES
C
PAN treatment
0h 2h 8h 24h
kDa
-15
IB: anti Cleaved Caspase 3/6 (D175)
-55
IB: anti b-Tubulin
Densitometry cl.casp/tubulin
PAN treatement
D
IDed
45
cuts (position)
not IDed
CASP3
CTSB
PMPCB
METAP2
CASP6
CASP9
CASP7
HNRNPH1
ALDOC
ENO1
ALDOA
EEF1A1P5
ATP5C1
SDHC
EEF2
PPIA
GAPDH
VIM
E
VIMENTIN
Epitope 1
Epitope 2
Domain structure
Filament
Regulation N-terminus (log2 PAN/veh)
P0(FL)
P1
P2
52kDa
42 kDa
25 kDa
Terminus in glomerulus
yes
yes
F
Epitope 1
Epitope 2
Veh.
PAN
kDa
-P0
-P1
-P2
Relative expression vs P0, a.u.
P1
P2
Veh
PAN

Fig. 3

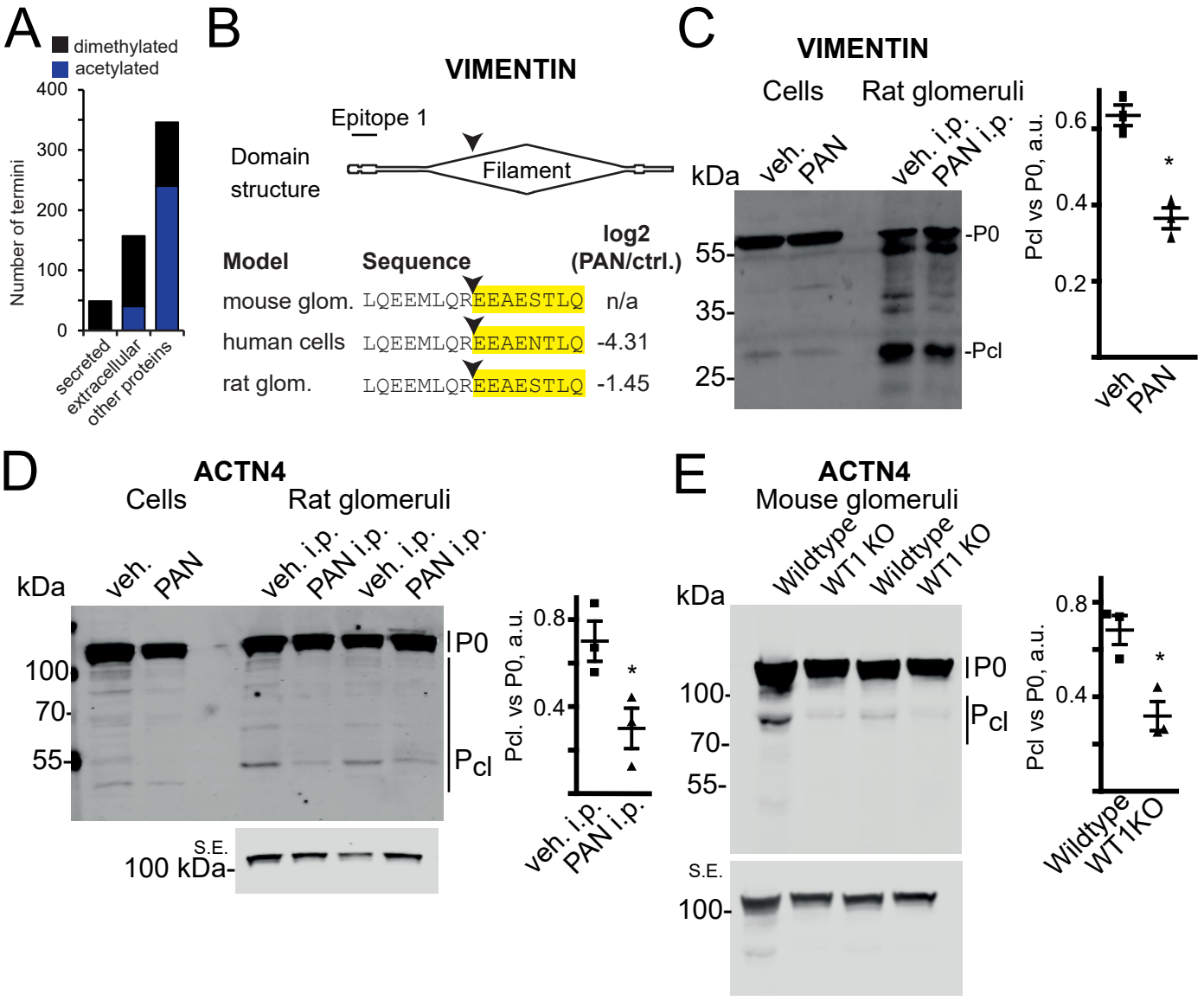
A
dimethylated
acetylated
Number of termini
400
300
200
100
0
secreted
extracellular
other proteins
B
VIMENTIN
Epitope 1
Domain
structure
Filament
Model
Sequence
log2
(PAN/ctrl.)
mouse glom. LQEEMLQREEAESTLQ n/a
human cells LQEEMLQREEAENTLQ -4.31
rat glom. LQEEMLQREEAESTLQ -1.45
C
VIMENTIN
Cells
Rat glomeruli
kDa
veh.
PAN
veh. i.p.
PAN i.p.
55
35
25
-P0
-Pcl
Pcl vs P0, a.u.
0.6
0.4
0.2
*
veh
PAN
D
ACTN4
Cells
Rat glomeruli
kDa
veh.
PAN
veh. i.p.
PAN i.p.
veh. i.p.
PAN i.p.
100
70
55
P0
Pcl
S.E.
100 kDa
Pcl. vs P0, a.u.
0.8
0.4
*
veh. i.p.
PAN i.p.
E
ACTN4
Mouse glomeruli
Wildtype
WT1 KO
Wildtype
WT1 KO
kDa
100
70
55
P0
Pcl
S.E.
100
Pcl vs P0, a.u.
0.8
0.4
*
Wildtype
WT1KO

Fig. 4

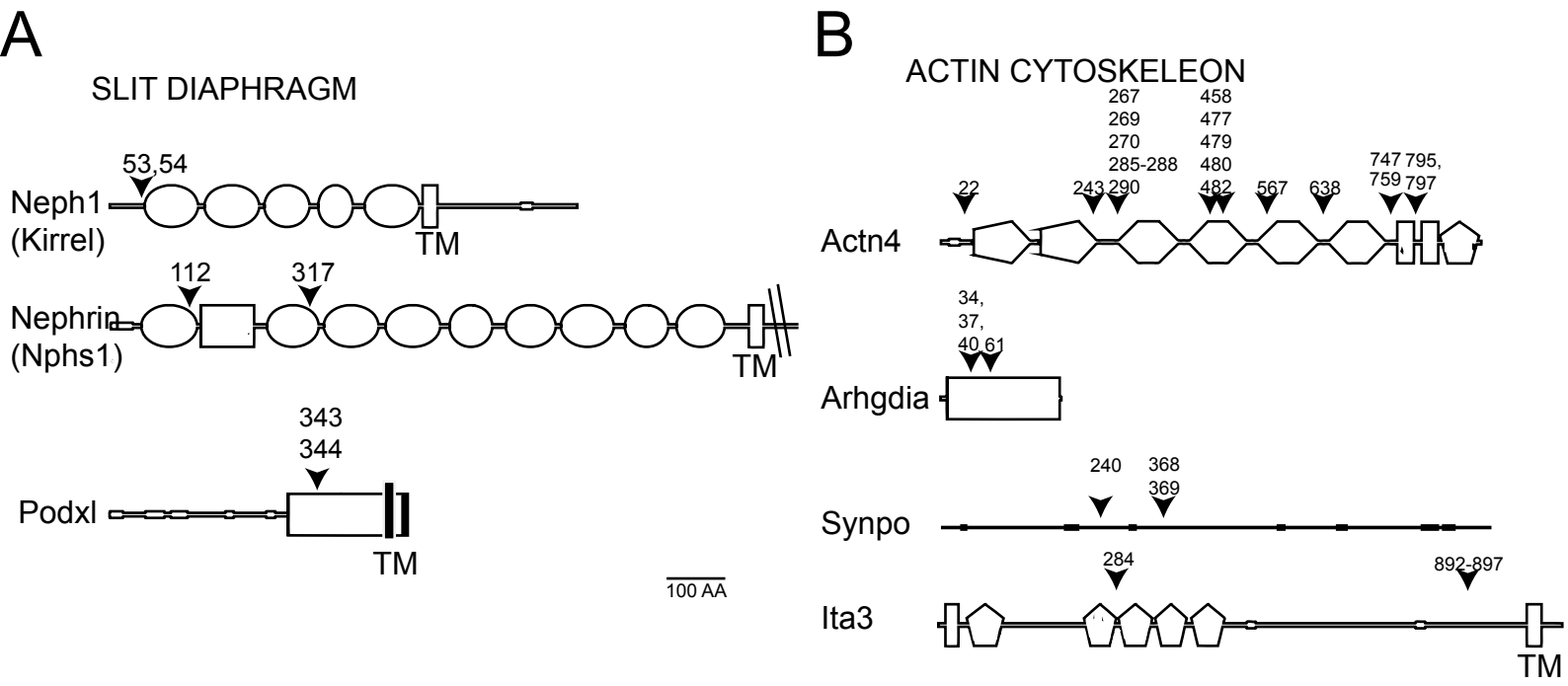
A
SLIT DIAPHRAGM
53,54
Neph1
(Kirrel)
TM
112
317
Nephrin
(Nphs1)
TM
343
344
Podxl
TM
100 AA
B
ACTIN CYTOSKELEON
267
269
270
285-288
458
477
479
480
22
243
290
482
567
638
747
759
795,
797
Actn4
34,
37,
40
61
Arhgdia
240
368
369
Synpo
284
892-897
Ita3
TM

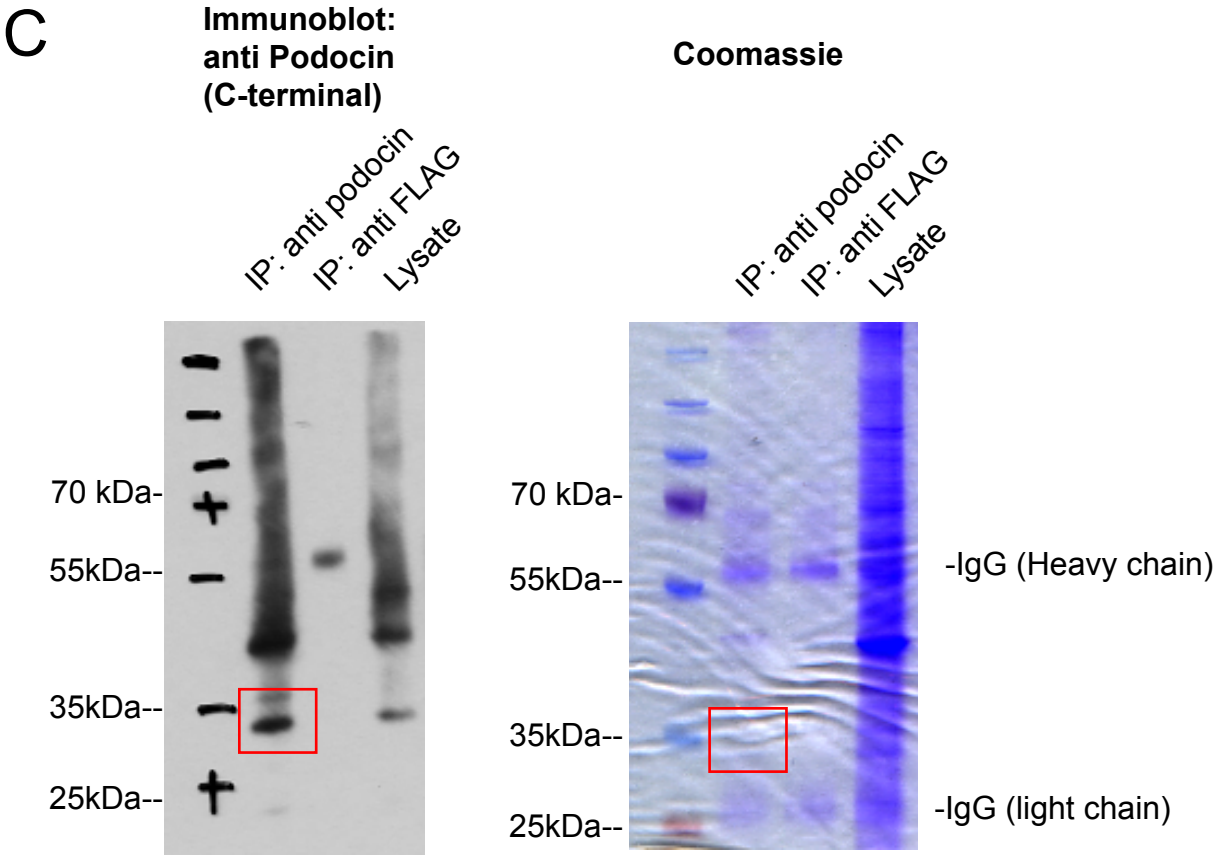
C
Immunoblot:
anti Podocin
(C-terminal)
IP: anti podocin
IP: anti FLAG
Lysate
70 kDa-
55kDa--
35kDa--
25kDa--
Coomassie
IP: anti podocin
IP: anti FLAG
Lysate
70 kDa-
55kDa--
35kDa--
25kDa--
-IgG (Heavy chain)
-IgG (light chain)

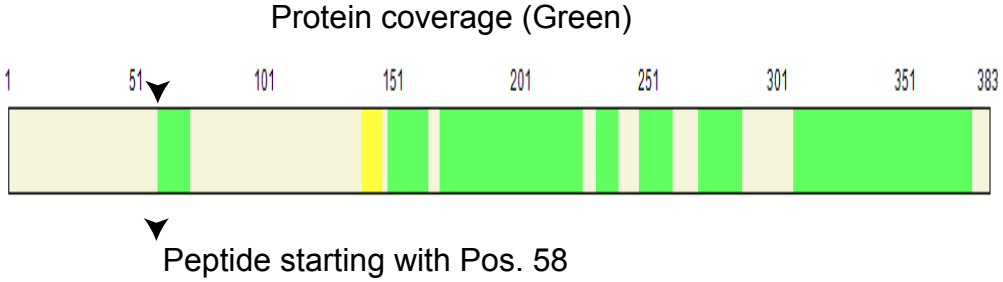
Protein coverage (Green)
1
51
101
151
201
251
301
351
383
Peptide starting with Pos. 58

Fig. S1

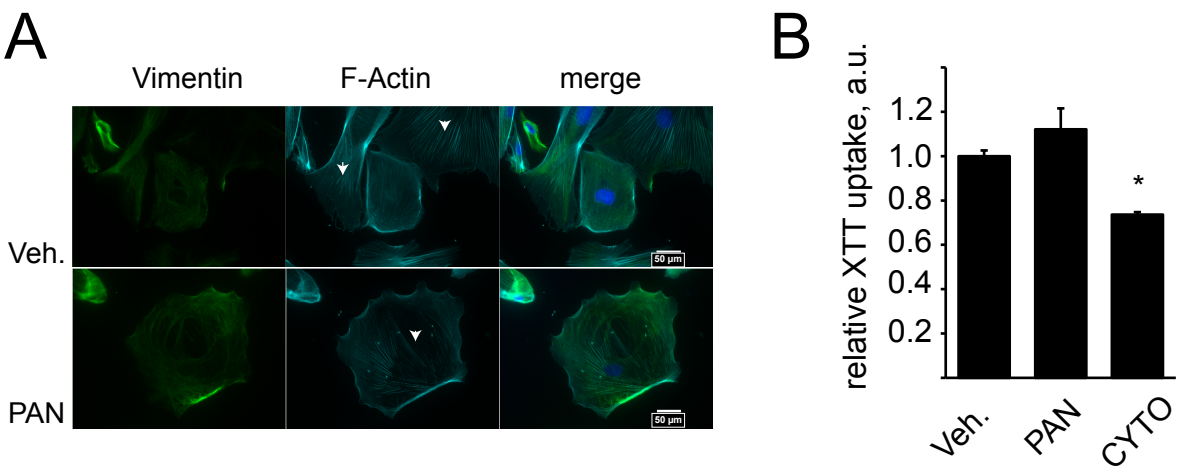
A
Vimentin
F-Actin
merge
Veh.
PAN
50 µm
50 µm
B
relative XTT uptake, a.u.
1.2
1.0
0.8
0.6
0.4
0.2
*
Veh.
PAN
CYTO

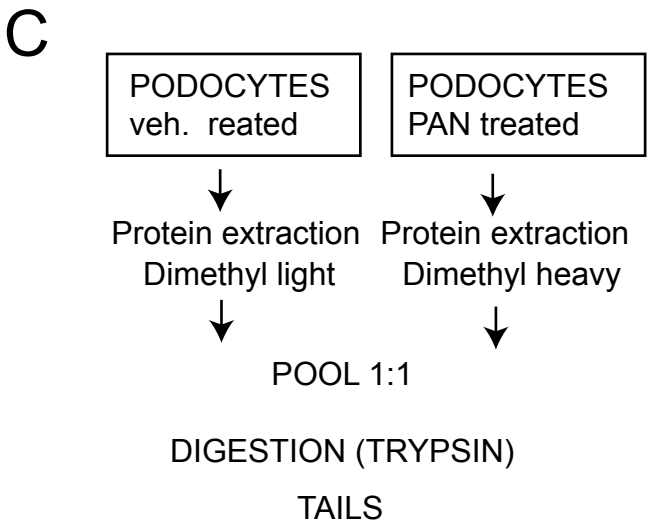
C
PODOCYTES
veh. reated
PODOCYTES
PAN treated
Protein extraction
Dimethyl light
Protein extraction
Dimethyl heavy
POOL 1:1
DIGESTION (TRYPSIN)
TAILS

Fig. S2

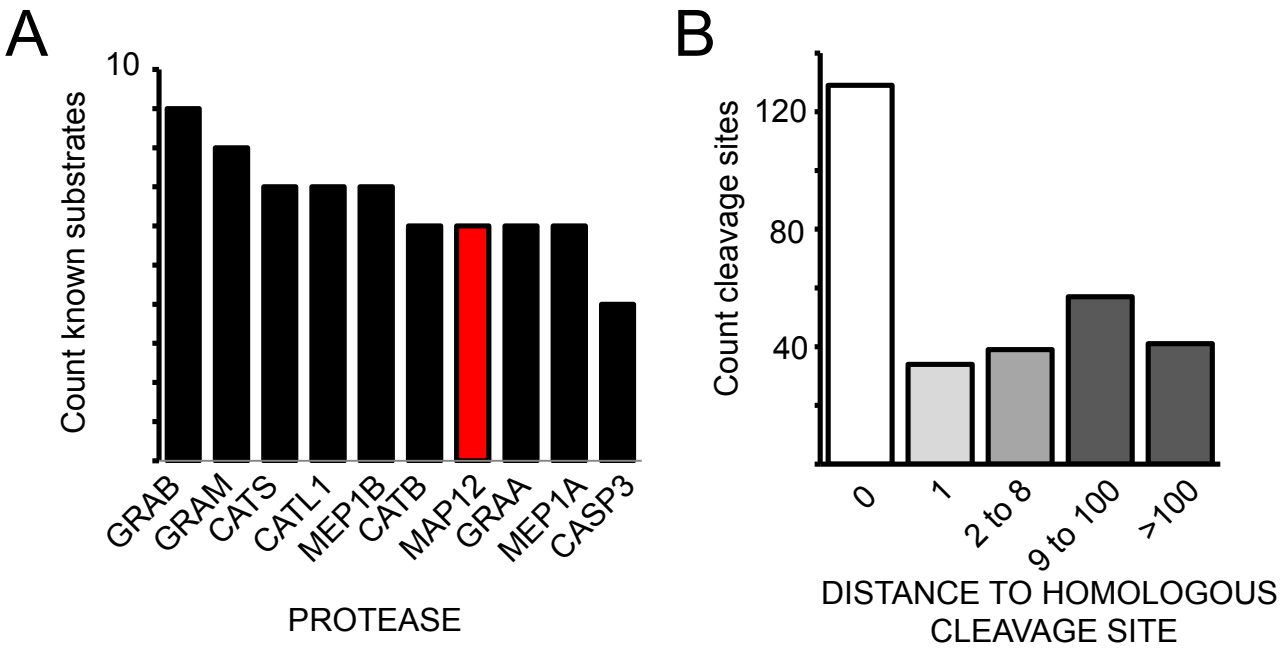
A
10
Count known substrates
GRAB
GRAM
CATS
CATL1
MEP1B
CATB
MAP12
GRAA
MEP1A
CASP3
PROTEASE
B
120
80
40
Count cleavage sites
0
1
2 to 8
9 to 100
>100
DISTANCE TO HOMOLOGOUS
CLEAVAGE SITE

Fig. S3

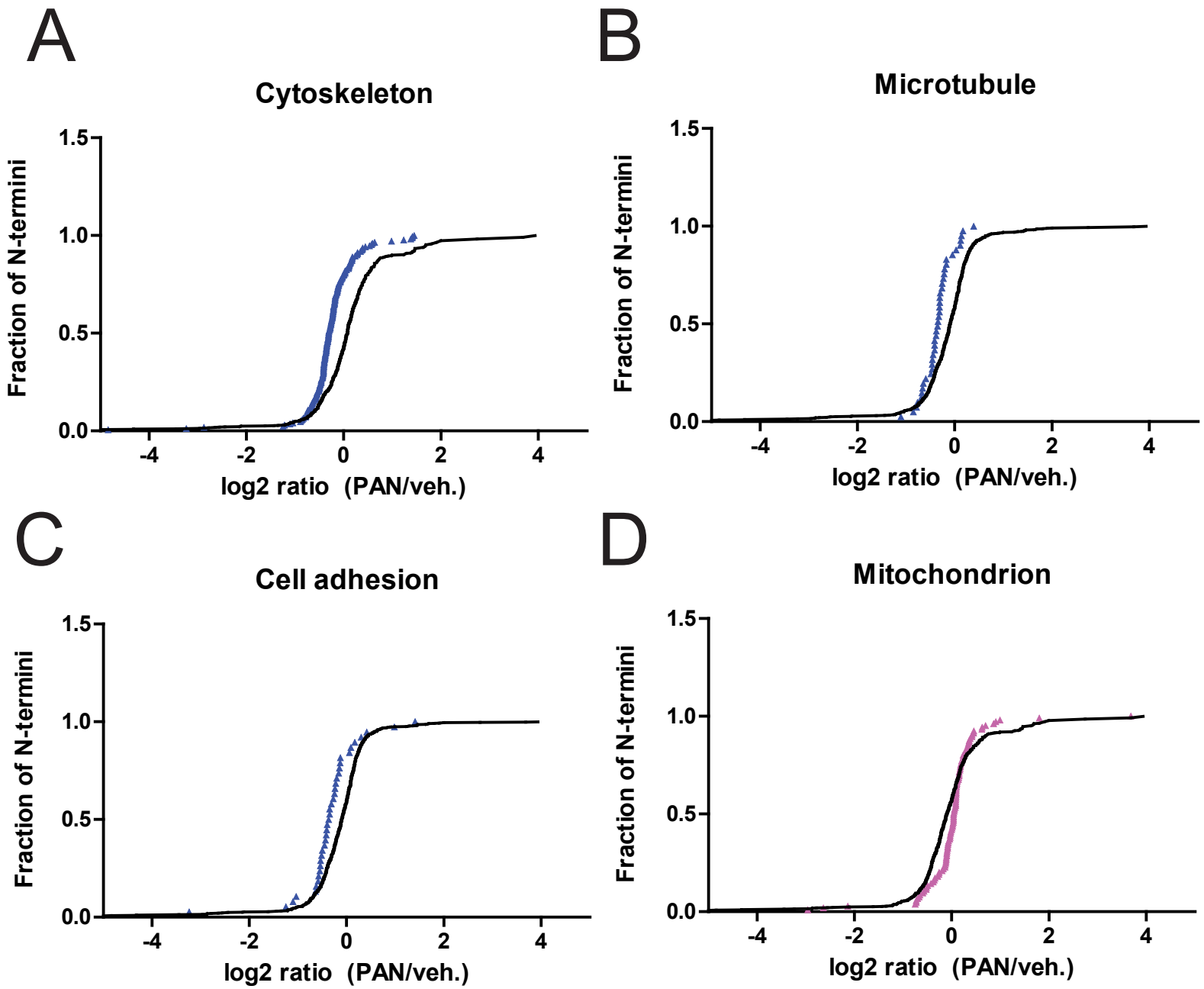
A
Cytoskeleton
Fraction of N-termini
1.5
1.0
0.5
0.0
-4
-2
0
2
4
log2 ratio (PAN/veh.)
B
Microtubule
Fraction of N-termini
1.5
1.0
0.5
0.0
-4
-2
0
2
4
log2 ratio (PAN/veh.)
C
Cell adhesion
Fraction of N-termini
1.5
1.0
0.5
0.0
-4
-2
0
2
4
log2 ratio (PAN/veh.)
D
Mitochondrion
Fraction of N-termini
1.5
1.0
0.5
0.0
-4
-2
0
2
4
log2 ratio (PAN/veh.)

Fig. S4

A

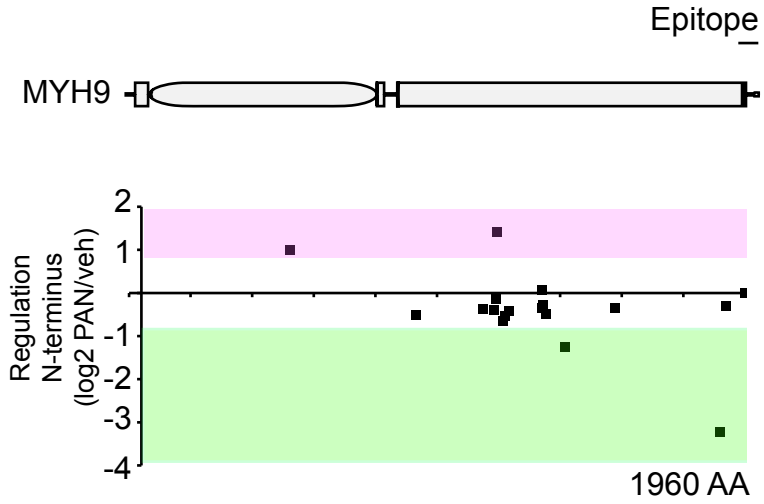
Epitope
MYH9
Regulation
N-terminus
(log2 PAN/veh)
2
1
-1
-2
-3
-4
1960 AA

B

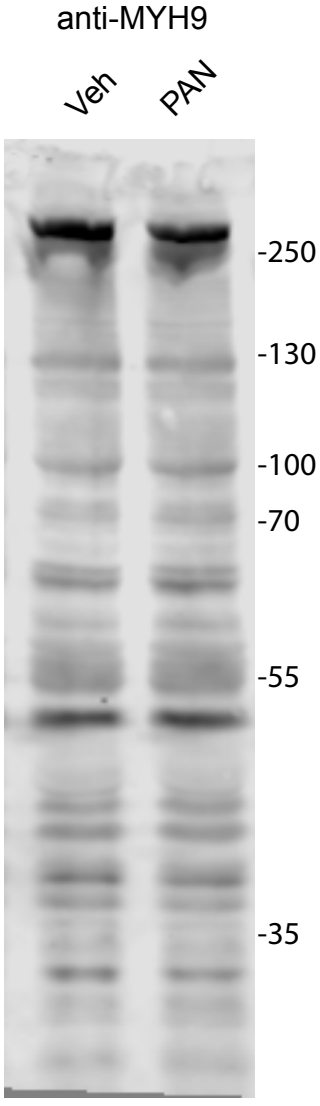
anti-MYH9
Veh
PAN
-250
-130
-100
-70
-55
-35

Fig. S5

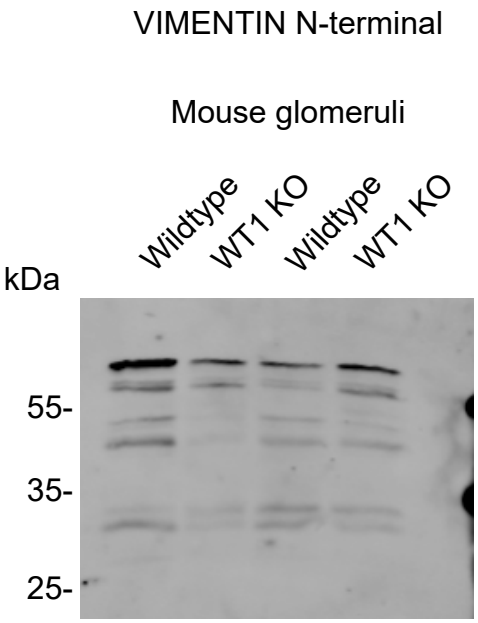
VIMENTIN N-terminal
Mouse glomeruli
Wildtype
WT1 KO
Wildtype
WT1 KO
kDa
55-
35-
25-

Fig. S6